

Complexation of *N'*-[1-(2,4-Dihydroxyphenyl)ethylidene]isonicotinohydrazide with Lanthanide Ions

Yuimi Varam* and Lonibala Rajkumari†

Department of Chemistry, Manipur University, Canchipur 795003, Manipur, India

 Supporting Information

ABSTRACT: The complexation of *N'*-[1-(2,4-dihydroxyphenyl)ethylidene]isonicotinohydrazide (DEH) with trivalent Pr, Nd, Gd, Tb, and Ho ions were studied employing potentiometric and spectroscopic techniques. The potentiometric studies carried out at different temperatures, (293.15, 303.15, and 313.15) K, in aqueous dioxane (30 %) medium at a constant ionic strength of $I = 0.1 \text{ mol} \cdot \text{dm}^{-3} \text{ KNO}_3$ indicate the presence of two ionizable protons in the ligand. The formation of Ln(III) complexes having 1:1 and 1:2 metal–ligand stoichiometry has been inferred from the metal–ligand formation curves and the elemental analysis data. The trend in the stability of the Ln(III) complexes follows the order: $\text{Pr} < \text{Nd} < \text{Gd} > \text{Tb} < \text{Ho}$. Thermodynamic parameters (ΔG , ΔH , and ΔS) of both protonation and complexation reactions are negative for all of the systems suggesting that the reactions are spontaneous, exothermic, and enthalpy-driven. A photoluminescence study reveals that the complexes are not luminescent due to the quenching effect of the ligand or aqueous or OH ions. The Tb(III) complex of the ligand isolated from ethanolic medium is paramagnetic, behaves as a 2:1 electrolyte, and is of 1:2 stoichiometry.

1. INTRODUCTION

Schiff bases of arylhydrazones derived from pyridine carboxylic acid hydrazides have attracted much attention from the chemists. The acid hydrazides $\text{R}-\text{CO}-\text{NH}-\text{NH}_2$ and their corresponding arylhydrazones $\text{R}-\text{CO}-\text{NH}-\text{N}=\text{CHR}$ have remarkable biological activity and a strong tendency to form chelates with transition, lanthanide, and main group metals. Their mode of chelation with metal ions have aroused interest in the past due to possible biomimetic applications.^{1,2} Hydrazones containing an active hydrogen component, when used as intermediates, can synthesize coupling products by using the azomethine $-\text{CONHN}=\text{CH}-$ group.^{3,4} Of the pyridine carboxylic acid hydrazides, isonicotinic acid hydrazide is a drug of proven therapeutic^{5,6} importance, and in many cases, an increase of such therapeutic effect was observed when the hydrazide was complexed with a metal ion.⁷ It has been reported^{8–10} that its hydrazones derived from condensation with aromatic aldehydes or ketones showed better antitubercular/antitumor activity. Metal complexes including lanthanide complexes of this and other hydrazones not only have interesting spectral and magnetic properties but also possess a diverse spectrum of biological and pharmaceutical activities.^{9,11–15}

The chelating behavior of Schiff bases formed by the condensation of isonicotinic acid hydrazides with heteroaromatic aldehydes and ketones have been studied^{16–19} in our laboratory to observe the influence that coordination exerts on their conformation or configuration, in connection with the nature of the metal, lanthanide ions in particular, and of the counterion. The interactions between such polydentate oxygen and nitrogen donor Schiff bases and trivalent lanthanide ions have always been related with anionic or proton ionizability of these ligands as they have the ability to displace more effectively the hydration sphere of the metal cation, providing more kinetically stable complexes. They have interested bioinorganic chemists for decades because

their interactions have served as model systems for the study of many bimolecular and metalloproteins. However, to understand the interactions and activities of these Schiff bases and their complexes, it is necessary to have detailed knowledge about the extent to which they bind to metal ions, the concentration of metal complexes in equilibrium mixture, and thermodynamic and solution equilibria involved in the reactions. These are conveniently obtained through the determination of stability constants.^{20,21}

Thus, as part of our ongoing research on the coordination properties of hydrazone ligands, we report here about the chelating abilities of a novel Schiff base, *N'*-[1-(2,4-dihydroxyphenyl)ethylidene]isonicotinohydrazide (DEH; Figure 1) with Pr^{3+} , Nd^{3+} , Gd^{3+} , Tb^{3+} , and Ho^{3+} ions through the determination of the stability constants potentiometrically and the calculation of thermodynamic data associated with the complexation reactions. Moreover, the ever-increasing use of lanthanides as potential luminescent materials^{22–29} and, for relatively simple instrumentation, to study the spectral properties of any novel lanthanide complex would be worthwhile. Therefore, we have also extended our studies to the luminescent behavior of the Tb(III) complex. We also discuss the possible coordinating behavior of the ligand toward the Ln^{3+} ions based on spectral data.

2. EXPERIMENTAL SECTION

2.1. Materials and Solutions. Isonicotinic acid hydrazide, 2,4-dihydroxyacetophenone, NaOH, KNO_3 , and 1,4-dioxane were obtained from E. Merck, Mumbai, and the metal salts, $\text{LnCl}_3 \cdot 6$

Received: April 15, 2011

Accepted: July 19, 2011

Published: August 10, 2011

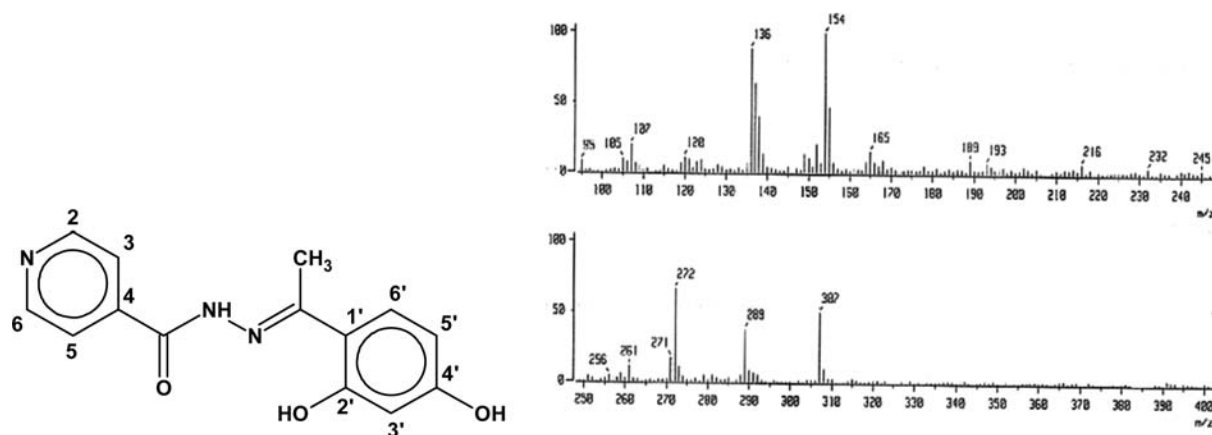


Figure 1. *N'*-[1-(2,4-Dihydroxyphenyl)ethylidene]isonicotinohydrazide (DEH) and its mass spectrum.

H₂O (Ln = Pr, Nd, Gd, Tb, Ho) were from Sigma-Aldrich, USA. All other chemicals used in this study were of analytical reagent (A.R.) grade. The metal salt solutions used for the potentiometric titrations were prepared in double-distilled water. Potassium hydroxide solution prepared in doubly distilled water was standardized with standard oxalic acid solution ($5 \cdot 10^{-2} \text{ mol} \cdot \text{dm}^{-3}$), which was again used for the standardization of HNO₃. The ligand solution ($5 \cdot 10^{-3} \text{ mol} \cdot \text{dm}^{-3}$) was prepared in a 30 % aqueous dioxane mixture.

2.2. Apparatus and Procedures. *Potentiometric Titration.* Potentiometric titration was carried out at three different temperatures, (293.15, 303.15 and 313.15) K, on a Cyberscan pH 1100 model with a glass calomel electrode, standardized with standard buffer solution of pH 4, 7, and 9 obtained from Eutech Instrument, Singapore. All of the titrations were carried out in a Dewar container and thermostatted with water circulated from a Circular D₈-G Haake Mess Technik to maintain the reaction mixture at the desired temperature.

Three sets of reaction mixtures were prepared, and the volume of each set was made up to 25 mL with double-distilled water.

Solution (a): 5 mL of KNO₃ ($0.10 \text{ mol} \cdot \text{dm}^{-3}$) + 2.5 mL of HNO₃ ($1 \cdot 10^{-3} \text{ mol} \cdot \text{dm}^{-3}$)

Solution (b): Solution (a) + 3 mL of DEH ($6 \cdot 10^{-4} \text{ mol} \cdot \text{dm}^{-3}$)

Solution (c): Solution (b) + 5 mL of Ln(III) ($3 \cdot 10^{-4} \text{ mol} \cdot \text{dm}^{-3}$)

Each set was titrated potentiometrically, adding aliquots of 20 μL of standard $5 \cdot 10^{-2} \text{ mol} \cdot \text{dm}^{-3}$ KOH solution at constant ionic strength maintained by $0.10 \text{ mol} \cdot \text{dm}^{-3}$ KNO₃ solution, keeping the metal–ligand molar ratio at 1:2. The titrations were repeated three times for each set. The equations of Irving and Rossotti^{30,31} were used to determine the stability constants of DEH and consequently used for the computation of formation constants of the complexes. The calculations were done by a personal computer using Microsoft Excel.

Luminescence Studies. The ethanolic solutions of TbCl₃·6 H₂O and ligand were prepared. The concentration of metal ion solution was kept constant ($5 \cdot 10^{-4} \text{ mol} \cdot \text{dm}^{-3}$), while the concentration of the ligand was varied according to the desired molar proportion in each recording. The spectra were recorded at room temperature.

2.3. Physical Measurements. C, H, and N were microanalyzed using a Perkin-Elmer model 240C, and the hydrazine content was estimated volumetrically, after subjecting the compound to acid hydrolysis for 4 h. Cl was estimated with a standard method.³² Tb(III) was estimated complexometrically using

xylene orange as an indicator.³³ The IR spectra were recorded in KBr medium on a Shimadzu FTIR-8400. The mass spectrum was obtained on a JEOL SX 102/Da-6000 mass spectrometer. NMR spectra were recorded on a JEOL AL 300 FT NMR spectrometer in DMSO. A Perkin-Elmer LS 55 fluorescence spectrophotometer was used for luminescent studies of Tb(III) and DEH. Molar conductance was measured on a CON 510 Conductivity/TDS/°C/F meter, Eutech Instruments, while the magnetic measurement was carried out using a magnetic susceptibility balance, Sherwood Scientific Ltd., UK, and thermal analysis on a Perkin-Elmer, STA 6000 simultaneous thermal analyzer purged with nitrogen gas.

2.4. Preparation and Characterization of Ligand. The ligand was prepared by refluxing ethanolic solutions of isonicotinic acid hydrazide (1.00 g in ~20 mL) and 2,4-dihydroxyacetophenone (1.65 g in ~30 mL) for ~4 h. The yellow precipitates obtained on cooling were filtered, washed with ethanol, and dried at room temperature. Yield = 55 %; mp, 272 °C; *M*⁺ peak appears at *m/z* = 272 as the base peak in the mass spectrum. (Figure 1).

Elemental Analysis of Ligand: Found % (Calcd % for C₁₄H₁₃N₃O₃). C, 61.68 (61.64); H, 4.67 (4.76); N, 15.43 (15.49); N₂H₄, 11.98 (11.80).

IR (*v*, cm⁻¹). 1660 (amide I), 1562 (amide II), 1610 (CN), 987 (NN), 3265(NH), 3165 (OH), 2940 (*v*_{as} CH₃), 2893 (*v*_s CH₃), 1226 (C–OH).

¹H NMR (δ). 13.384 (s, C2'-OH), 11.418 (s, C4'-OH), 10.928 (s, NHCO), 2.416 (s, CH₃), 8.782–7.825 (m, pyridine ring protons), 7.48–6.275 (m, phenyl ring protons).

¹³C NMR (*ppm*). 170.52, (s, CO), 166.55 (s, C2'), 152.94 (s, C4'), 149.48 (NC), 143.85(s, C4), 136.85, 131.34, 124.25, 119.65 (C6', C1', C5', C3' of phenyl ring, respectively), 128.32, 127.24 (C2, C3 of pyridine ring, respectively), 65.21 (s, CH₃).

Synthesis of the Tb(III)-DEH Complex. The complex was synthesized by refluxing the ethanolic solutions of the metal chlorides (1 g in ~20 mL) and DEH (2.06 g in ~40 mL) in 1:2 molar proportions for ~6 h and isolated from the concentrated reaction mixture using acetonitrile. It was then suction-filtered and dried in a desiccator. Yield = 60 %.

3. RESULTS AND DISCUSSION

3.1. Titration Curves. Potentiometric titrations of the ligand with Pr(III), Nd(III), Gd(III), Tb(III), and Ho(III) were carried

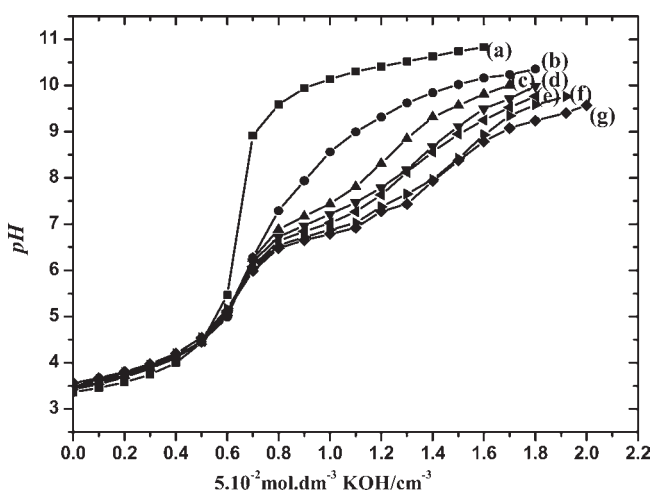


Figure 2. Titration curves of Ln(III) DEH complexes at 303.15 K and $I = 0.10 \text{ mol} \cdot \text{dm}^{-3} \text{ KNO}_3$; (a) 5 mL of $0.10 \text{ mol} \cdot \text{dm}^{-3} \text{ KNO}_3 + 2.5 \text{ mL}$ of $1 \cdot 10^{-3} \text{ mol} \cdot \text{dm}^{-3} \text{ HNO}_3$; (b) solution (a) + 3 mL of $6 \cdot 10^{-4} \text{ mol} \cdot \text{dm}^{-3} \text{ DEH}$; (c) solution (b) + 5 mL of $3 \cdot 10^{-4} \text{ mol} \cdot \text{dm}^{-3} \text{ Pr(III)}$; (d) solution (b) + 5 mL of $3 \cdot 10^{-4} \text{ mol} \cdot \text{dm}^{-3} \text{ Nd(III)}$; (e) solution (b) + 5 mL of $3 \cdot 10^{-4} \text{ mol} \cdot \text{dm}^{-3} \text{ Tb(III)}$; (f) solution (b) + 5 mL of $3 \cdot 10^{-4} \text{ mol} \cdot \text{dm}^{-3} \text{ Ho(III)}$; (g) solution (b) + 5 mL of $3 \cdot 10^{-3} \text{ mol} \cdot \text{dm}^{-3} \text{ Gd(III)}$.

out with standard KOH at $I = 0.10 \text{ mol} \cdot \text{dm}^{-3} \text{ KNO}_3$ and at three different temperatures, (293.15, 303.15, and 313.15) K, in 30 % aqueous dioxane solution. Figure 2 represents the potentiometric equilibrium curves of the acid titration curve (a), ligand titration curve (b), and the complex curves (c–g) at 303.15 K. Similar curves were obtained for titrations at other temperatures. The acid titration curve started from pH 3.3 and extended to pH 10.9. At the initial stage of the titration curve (pH range 3.2 to 4.2), the ligand curve is shifted to the left of the acid curve due to the basic properties of the ligand. The ligand may accept a proton in the strongly acidic medium. The acid curve and the ligand curve converged and started diverging from pH 4.5 to 4.7 which is due to the liberation of the proton from the ligand at these pH ranges.

It is observed that the complex curves almost coincided with the ligand curve in the initial stage and started diverging at the pH range 6.0 to 6.5. This indicates the liberation of proton from DEH due to the formation of the respective metal complexes. The decrease in pH for the metal titration curves relative to the ligand titration curve can be attributed to the formation of metal ligand bonding.³⁴ The color of the titrates after complex formation was found to be different from that of the ligand at the same pH. In the titrations, low concentrations of the metals have been used to preclude the formation of polynuclear complexes. The complex curves show two inflections corresponding to the formation of two types of complexes.

3.2. Proton–Ligand Formation Constant. The average number of protons, \bar{n}_H , bound to the ligand was calculated using relation 1

$$\bar{n}_H = Y - \frac{(V_L - V_A)(N + E^0)}{(V_0 + V_A)T_L^0} \quad (1)$$

where Y is the number of dissociable protons present in the ligand, V_L and V_A are the volumes of KOH added to ligand and acid solutions, respectively, for the same pH reading, V_0 is the initial volume of the reaction mixture, and E^0 and T_L^0 are the

concentrations of acid and ligand in the reaction mixture, respectively.

The proton–ligand formation curves extending from 0.3 to 1.9 on the \bar{n}_H scale for the systems at temperatures of (293.15, 303.15, and 313.15) K (Figure 3a) obtained by plotting \bar{n}_H versus pH show that two protons are dissociating from the ligand. The protonation constants, $\log K_{1(\text{DEH})}^H$ and $\log K_{2(\text{DEH})}^H$, at different temperatures were evaluated from the curves using Bjerrum's half integral method³⁴ and are collected in Table 2. Hydrazones containing azomethine are reported^{9,12,35} to exhibit keto–enol tautomerism and deprotonate the amido proton at high pH. Therefore, DEH is also expected to exhibit keto–enol tautomerism, and the amido proton would be dissociated from the ligand through enolization as illustrated (Supporting Information, Figure 2). DEH loses the enolic proton at higher pH, and the first protonation constant, $\log K_{1(\text{DEH})}^H$, may correspond to its dissociation. Of the two phenyl protons, the deprotonation of the ortho-OH proton of the phenyl ring will be favored in the presence of some electron-withdrawing substituent, and its dissociation may correspond to $\log K_{2(\text{DEH})}^H$. The dissociation of the para-OH proton of the phenyl ring is ruled out in the working medium and at the working pH range and may be feasible only at higher pH. The deprotonation of DEH is dependent on temperature and decreases with an increase in temperature, showing that the process is more favorable at low temperatures.³⁶

3.3. Metal–Ligand Formation Constant. The average number of ligands attached per metal ion (\bar{n}) and the free ligand exponent (pL) were calculated from the potentiometric data using relations 2 and 3.

$$\bar{n} = \frac{(V_M - V_L)(N + E^0)}{(V_0 + V_A)T_M^0 \bar{n}_H} \quad (2)$$

and pL, the free ligand exponent, was given by

$$\text{pL} = \log_{10} \left[\frac{\sum_{n=0}^{n=j} \beta_n H \left(\frac{1}{\text{antilog pH}} \right)^n}{T_L^0 - \bar{n} T_M^0} \cdot \frac{V_0 + V_M}{V_0} \right] \quad (3)$$

V_M is the volume of alkali added to metal solution at the same pH reading as that of V_A , $\beta_n H$ is the overall protonation constant of the ligand, and T_M^0 is the concentration of Ln(III) in the metal solutions. Other symbols have their usual significance as in eq 1. The metal ligand formation curves were obtained by plotting the values of \bar{n} against pL for different temperatures, and the formation curves at 303.15 K are represented in Figure 3b.

The stepwise formation constants, $\log K_{2(\text{DEH})}^{\text{Ln}}$ and $\log K_{1(\text{DEH})}^{\text{Ln}}$, were evaluated from the formation curves employing Bjerrum's half integral method³⁴ and are given in Table 1. The values of \bar{n} ($0.20 < \bar{n} < 1.5$) indicate that the complexes formed are of 1:1 and 1:2 metal–ligand stoichiometry. There is a gradual decrease of the values of the stability constants with increasing temperature, showing that the complex formation process is exothermic and more favorable at lower temperatures. The difference between $\log K_{1(\text{DEH})}^{\text{Ln}}$ and $\log K_{2(\text{DEH})}^{\text{Ln}}$ in Table 1 are all positive, meaning that the coordination of the first ligand to the metal is more favorable than that of the second ligand molecule.

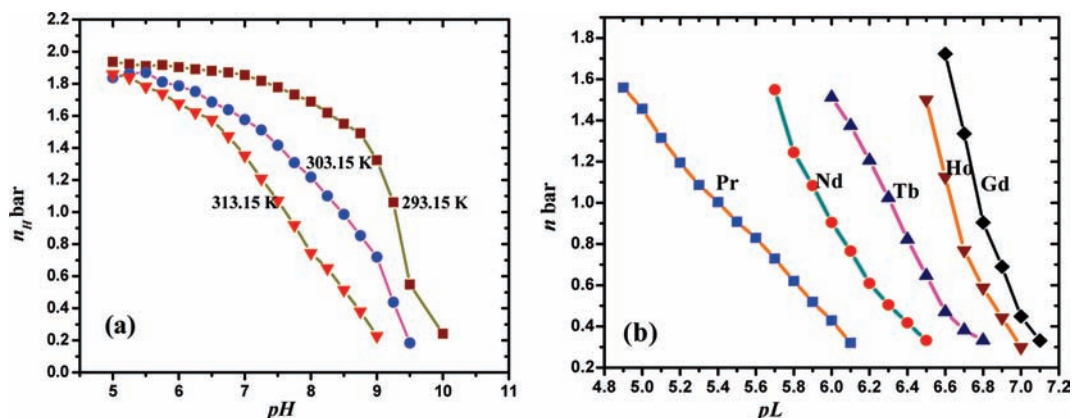


Figure 3. (a) Proton–ligand formation curves of DEH at different temperatures. (b) Metal–ligand formation curves of Ln(III) DEH complexes at 303.15 K.

Table 1. Stepwise Metal–Ligand Formation Constants, $\log K_{1(\text{DEH})}^{\text{Ln}}$ and $\log K_{2(\text{DEH})}^{\text{Ln}}$, and Overall Formation $\log \beta_{\text{DEH}}^{\text{Ln}}$ of Ln(III) DEH Complexes and $I = 0.10 \text{ mol} \cdot \text{dm}^{-3} \text{ KNO}_3$ at Different Temperatures in Aqueous Dioxane Media^a

T		metal ions				
K	formation constant	Pr	Nd	Gd	Tb	Ho
293.15	$\log K_{1(\text{DEH})}^{\text{Ln}}$	7.81 ± 0.06	8.40 ± 0.09	8.65 ± 0.08	8.71 ± 0.06	8.74 ± 0.05
	$\log K_{2(\text{DEH})}^{\text{Ln}}$	4.97 ± 0.06	6.30 ± 0.09	8.04 ± 0.08	7.60 ± 0.06	7.68 ± 0.05
	$\log \beta_{\text{DEH}}^{\text{Ln}}$	12.78 ± 0.06	14.70 ± 0.09	16.69 ± 0.08	16.31 ± 0.06	16.42 ± 0.05
303.15	$\log K_{1(\text{DEH})}^{\text{Ln}}$	5.92 ± 0.05	6.04 ± 0.04	6.98 ± 0.05	6.59 ± 0.08	6.87 ± 0.1
	$\log K_{2(\text{DEH})}^{\text{Ln}}$	4.97 ± 0.05	5.72 ± 0.04	6.66 ± 0.05	6.00 ± 0.08	6.48 ± 0.1
	$\log \beta_{\text{DEH}}^{\text{Ln}}$	10.89 ± 0.05	11.76 ± 0.04	13.64 ± 0.05	12.60 ± 0.08	13.34 ± 0.1
313.15	$\log K_{1(\text{DEH})}^{\text{Ln}}$	4.58 ± 0.11	5.18 ± 0.11	5.79 ± 0.02	5.46 ± 0.02	5.56 ± 0.1
	$\log K_{2(\text{DEH})}^{\text{Ln}}$	4.08 ± 0.11	4.85 ± 0.11	5.29 ± 0.02	5.12 ± 0.11	5.17 ± 0.1
	$\log \beta_{\text{DEH}}^{\text{Ln}}$	8.67 ± 0.11	10.03 ± 0.11	11.08 ± 0.02	10.57 ± 0.11	10.74 ± 0.1

^a ± values are the standard deviations.

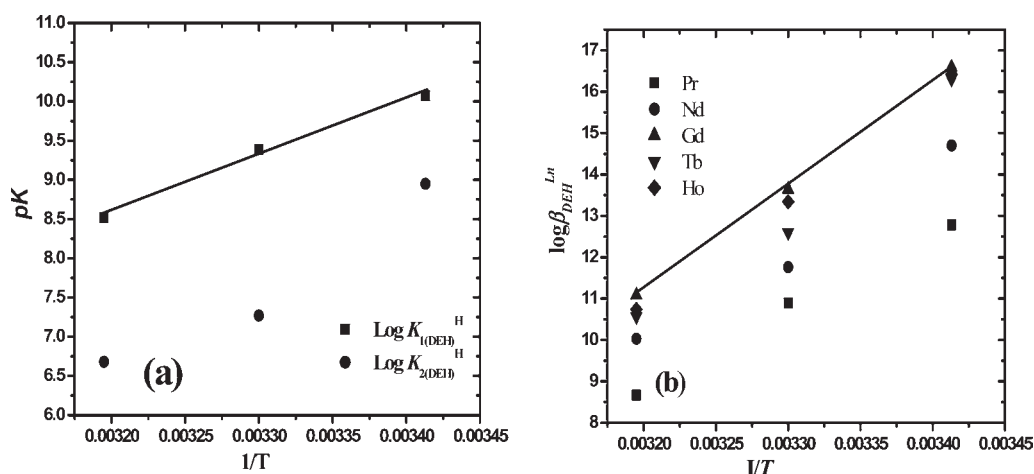


Figure 4. van't Hoff plot of pK for dissociation of (a) DEH and (b) Ln(III)-DEH complexes against $1/T$.

At constant temperature, the trend in the formation constants, $\log \beta_{\text{DEH}}^{\text{Ln}}$ of the metal chelates is: Pr(III) < Nd(III) < Gd(III) > Tb(III) < Ho(III). The higher stability of Gd(III) complex is not uncommon for the complexes of the lanthanide series.^{37–39} A plot of $\log \beta_{\text{DEH}}^{\text{Ln}}$ versus $1/r$ (Figure 3 of the Supporting Information) indicates that the stability constants of metal chelates generally increase with the increase in atomic number.

3.4. Effect of Temperature. The change in free energy (ΔG) was calculated from the formation constant values ($\log K$) at various temperatures using the following equation:

$$\Delta G = -2.303RT \log K \quad (5)$$

Table 2. Thermodynamics Parameters^a of Dissociation of DEH in 30 % (v/v) Aqueous Dioxane Medium in the Presence of 0.10 mol·dm⁻³ KNO₃ Solution at 303.15 K

T/K	log K _{1(DEH)} ^H	log K _{2(DEH)} ^H	-ΔG ₁	-ΔG ₂	-ΔH ₁	-ΔH ₂	-ΔS ₁	-ΔS ₂
293.15	10.07 ± 0.05	8.95 ± 0.0	56.52	50.23	135.87 ± 0.08	200.46 ± 0.43	0.63 ± 0.08	0.80 ± 0.43
303.15	9.39 ± 0.01	7.27 ± 0.01	54.47	42.18				
313.15	8.52 ± 0.02	6.68 ± 0.02	51.08	40.05				

^a ΔG and ΔH = (kJ·mol⁻¹); ΔS = (kJ·K⁻¹·mol⁻¹).

Table 3. Thermodynamics Parameters^a of Ln(III) DEH Complexes at 303.15 K and I = 0.10 mol·dm⁻³ KNO₃ in 30 % (v/v) Aqueous Dioxane Medium

Ln(III)-DEH complexes	-ΔG ₁	-ΔG ₂	-ΔH ₁	-ΔH ₂	-ΔS ₁	-ΔS ₂
Pr	34.33	28.85	284.16 ± 0.17	77.18 ± 0.37	1.05 ± 0.17	0.34 ± 0.37
Nd	35.04	33.18	284.29 ± 0.56	126.98 ± 0.14	1.05 ± 0.56	0.53 ± 0.14
Gd	40.49	38.64	251.59 ± 0.04	241.42 ± 0.03	0.96 ± 0.04	0.92 ± 0.03
Tb	38.23	34.81	286.38 ± 0.35	218.49 ± 0.09	1.07 ± 0.35	0.83 ± 0.09
Ho	39.86	37.59	279.00 ± 0.18	220.24 ± 0.08	1.05 ± 0.18	0.85 ± 0.08

^a ΔG and ΔH = (kJ·mol⁻¹); ΔS = (kJ·K⁻¹·mol⁻¹). ΔH and ΔS were calculated using the linear fit program.

where *R* (ideal gas constant) = 8.314 J·K⁻¹·mol⁻¹; *K* = protonation constant of DEH or stability constant of the complexes; *T* = absolute temperature. The enthalpy change (Δ*H*) for the dissociation of DEH and complexation process was evaluated from the slope of the plot log *K*_{n(DEH)}^H or log β_{DEH}^{Ln} versus 1/*T*, (Figure 4a,b) using the graphical representation of van't Hoff's eq 6, and the change in entropy (Δ*S*) could then be calculated using relationship 7:

$$\Delta G = \Delta H - T\Delta S \quad (6)$$

$$\Delta S = (\Delta H - \Delta G)/T \quad (7)$$

The data thus calculated for protonation and complexation reactions of DEH are given in Tables 2 and 3, respectively. All of the thermodynamic parameters are negative indicating that all the reactions are spontaneous, exothermic, and enthalpy-driven. The unfavorable change of entropy (negative Δ*S*) may be due to extensive solvation of metal chelates in aqueous organic medium.⁴⁰ It is also likely to be contributed by the loss of rotational entropy of the phenyl ring with the rest of the molecule, >N–N< and N–C bond linkage of DEH, once complexation had taken place. The thermodynamic parameters of the complexes when correlated with the reciprocal ionic radii of the lanthanides, 1/*r*, show that generally free energy (Δ*G*) and enthalpy (Δ*H*) increase, while entropy (Δ*S*) decreases with a decrease in ionic radii of the lanthanides. It is therefore apparent that the Ln(III) complexes of DEH are stabilized by favorable enthalpy.

4. PHOTOLUMINESCENCE STUDY OF THE Tb(III)-DEH COMPLEX

Tb(III) emission can be greatly enhanced upon complexation or when bound to a chelator. If the chelator contains suitable chromophore, an emission enhancement of several orders of magnitudes can be observed due to favorable energy transfer. Unlike the extremely low absorptivity of the lanthanides, the sensitizers (chromophore) typically have high molar extinction coefficients.⁴¹

The emissions of Tb(III) corresponding to ⁵D₄–⁷F₆, ⁵D₄–⁷F₅, ⁵D₄–⁷F₄, and ⁵D₄–⁷F₃ transitions²⁹ were clearly observed when excited at 220 nm in ethanolic medium. They are not significant when the ion is excited at (250, 280) nm (Figure SII) and (270, 330) nm (not shown in the figure). In the presence of DEH, the excitation and emission spectra of the Tb(III) ion show a significant difference (Figures SI,II and 6), and this indicates complexation or some kind of interaction between them. Encapsulation of Tb(III) ion by various possible chelators of DEH would have increased the emission quantum yield when compared to the free metal ion. But all of the emission peaks of terbium get quenched, and a broad band in the (485 to 500) nm of low intensity appears in the spectrum which may be the remnant ⁵D₄–⁷F₆ peak. Though observed almost at the same frequency [(485 to 500) nm], the intensity of the bands are different for varying metal–ligand molar ratio, which is at a maximum for a 1:0.0 M/L molar ratio and becomes weaker for 1:2 to 1:3 M/L ratios.

The quenching may be due to the presence of OH oscillators in the coordinated water molecules, ligand, and in the solvent that are generally more effective nonradiative relaxers of the ⁵D₄ excited states than are other ligand or ligand donor groups.^{42–44} The quenching effect is directly proportional to the number of water molecules (OH oscillator) both in the inner coordination sphere (to a larger extent) and outer coordination sphere⁴⁵ (to a smaller extent) and to N–H vibrators.^{45,46} Some of the water molecules which were hitherto present in the metal chlorides as lattice water must have coordinated to the central metal atom in the complex. Thus, through the presence of the high frequency OH, NH, or CH (contribution negligible) oscillators present in the complex, deactivation of the emissive levels of the metal ion by vibronic coupling (intensity and lifetime)⁴⁷ may have taken place. This will greatly diminish terbium luminescence. The ligand, therefore, has no sensitizing effects but rather quenches Tb(III) luminescence in ethanolic solution.

4.1. Outer Versus Inner Sphere Complex. Choppin et al.⁴⁸ proposed the use of thermodynamic parameters for the evaluation of inner sphere versus outer sphere complexation. High negative Δ*H* and negative Δ*S* obtained for complexation reactions would suggest the formation of outer sphere complex. However, on the

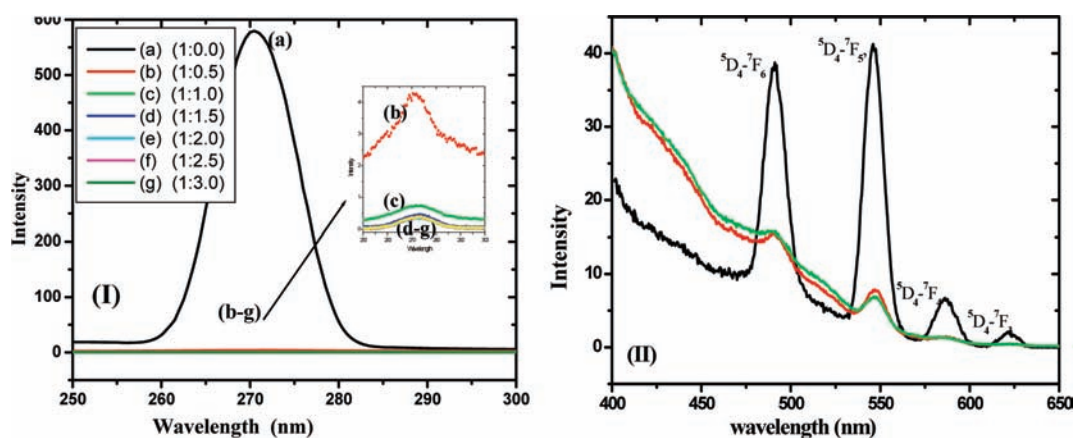


Figure 5. (I) $\lambda_{\text{ex}} = 545 \text{ nm}$, ${}^5\text{D}_4\text{-}{}^7\text{F}_5$, excitation spectra of the $5 \cdot 10^{-4} \text{ mol} \cdot \text{dm}^{-3}$ Tb(III) ion (concentration constant) and DEH (concentration variable) at different M:L molar proportions. Inset: enlargement of the spectra excluding 1:0 M/L molar ratios. (II) Emission spectra of the $5 \cdot 10^{-4} \text{ mol} \cdot \text{dm}^{-3}$ Tb(III) ion monitored at different excitations of 220 nm (black line), 250 nm (red line), and 280 nm (green line) in ethanolic medium.

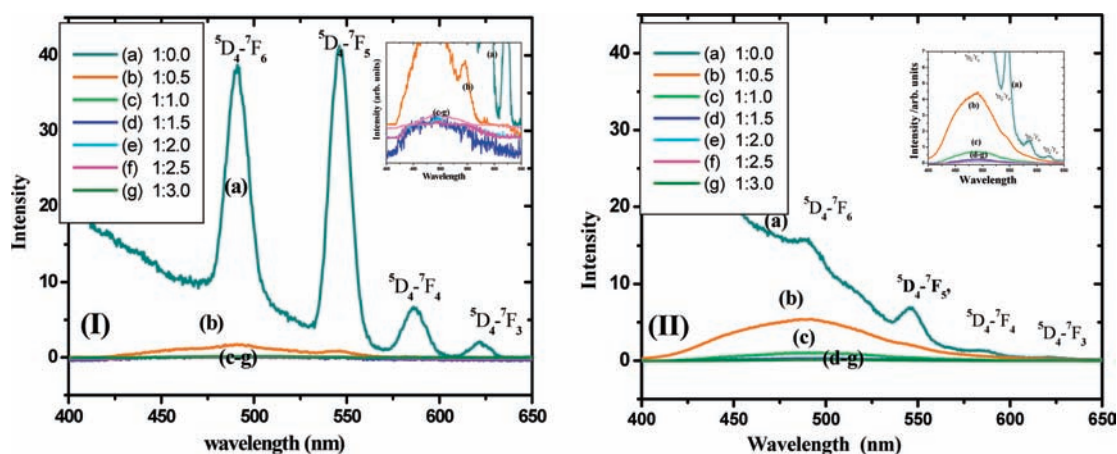


Figure 6. Emission spectra of the $5 \cdot 10^{-4} \text{ mol} \cdot \text{dm}^{-3}$ Tb(III) ion (concentration constant) and DEH (concentration variable) at different metal–ligand molar ratios monitored at (I) 220 nm and (II) 280 nm. Insets: enlargement of spectra excluding 1:0 molar ratios.

Table 4. Analytical Data and Physical Properties of DEH and $\text{Tb}[(\text{DEH})_2(\text{H}_2\text{O})_2\text{Cl}]\text{Cl}_2 \cdot 3\text{H}_2\text{O}$

ligand/complex	color	mp ($^{\circ}\text{C}$)	found (calcd)%						
			Tb	N_2H_4	C	H	N	Cl	
DEH	yellow	272		11.98 (11.80)	61.68 (61.64)	4.67 (4.76)	15.43 (15.45)		
$\text{Tb}[(\text{DEH})_2(\text{H}_2\text{O})_2\text{Cl}]\text{Cl}_2 \cdot 3\text{H}_2\text{O}$	yellow	116 ^a	18 (18)	9.04 (8.69)	38.23 (38.22)	3.98 (3.86)	9.49 (9.56)	12.18 (12.16)	

^a Decomposition temperature.

basis of the changes in the excitation and luminescence spectra, the formation of both the inner and outer sphere complexes is highly probable.⁴⁹ The interaction between the ligand and Tb(III) may be of both coordinated and weak interactions and most probably exist as a mixture of inner sphere and outer sphere complex at room temperature in ethanolic medium.

5. TB(III)-DEH COMPLEX

The analytical data of Tb(III)-DEH complex are given in Table 4. The complex is yellow-colored, stable, and nonhygroscopic. It is

soluble in water and common organic solvents. The room temperature magnetic moment of complex is $9.22 \mu_{\text{B}}$ which is in the expected range for paramagnetic f^8 configuration of the Tb^{3+} ion. The molar conductance value, $86 \Omega \cdot \text{cm}^2 \cdot \text{mol}^{-1}$, indicates that the complex behaves as a 2:1 electrolyte in $1 \cdot 10^{-3} \text{ mol} \cdot \text{dm}^{-3}$ ethanolic.⁵⁰

The thermogravimetric (TGA) curve of the Tb(III) complex with DEH indicates the presence of five water molecules, as shown by the decomposition curve in the (100 to 200) $^{\circ}\text{C}$ range. Although decomposed fragments of the ligand could not be estimated due to continuous weight loss, the complete

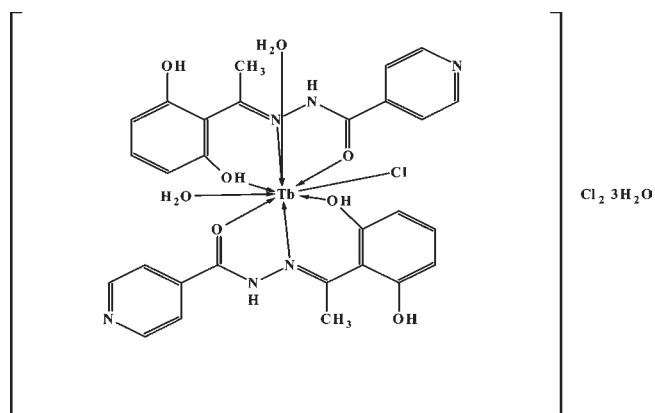


Figure 7. Structure of $[Tb(DEH)_2(H_2O)_2Cl]Cl_2 \cdot 3H_2O$.

decomposition of ligand occurs at ~ 900 °C. The gradual loss in weight with increasing temperature from (200 to 900) °C corresponds to the decomposition of the two ligand molecules and chlorine present in the complex. The zone beyond 900 °C or the weights that still remain suggest the ultimate product, which in the nitrogenized atmosphere corresponds to TbN_3 . The differential thermal (DTA) curve shows one endothermic peak at 116 °C, tallying with the loss of water molecules from the complex. An exothermic peak at 560 °C may be due to the phase change such as crystallization or the transition between different crystal structures or because of some chemical reactions.

The IR spectrum of DEH in KBr medium exhibits an absorption band at 1660 cm^{-1} due to (C=O) of the pyridyl moiety. The band shifts to 1654 cm^{-1} in the complex. This indicates the coordination of the ligand with the metal ion through the carbonyl group of the pyridyl moiety. Shifts of the C–OH stretching vibration of the phenolic part from (1226 to 1203) cm^{-1} support the coordination through the phenolic oxygen which is also favorable due to the possible formation of highly stable six membered chelates. The ligand band at 987 cm^{-1} due to (N–N) undergoes a (20 to 30) cm^{-1} hypsochromic shift upon complexation to 1008 cm^{-1} . The magnitude of this positive shift indicates the monodentate linking of the $>N-N<$ residue.⁵¹ The bonding through oxygen and nitrogen are further supported by the appearance of new bands at (580 and 416) cm^{-1} and assignable to (M–O) and (M–N) vibrations, respectively.⁵¹ Thus, the bonding sites can be inferred in the Tb(III)-DEH complex.

6. HYDRATION NUMBER OR COORDINATED WATER

The presence of water molecules suggested from the IR spectra and photoluminescence quenching was confirmed by TGA studies. It demonstrates the presence of five water molecules. Tb(III) generally has a coordination number of nine in its complexes. On that basis, two water molecules may be coordinated with the central metal ion within the inner coordination sphere, the remaining six coordination sites being occupied by the two ligands as is evident from IR spectra and a chlorine atom. The remaining three water molecules are therefore assigned outside the coordination sphere.

From the above spectral and physicochemical data, the structure of the complex may be tentatively assigned as shown in Figure 7.

7. CONCLUSION

A potentiometric study reveals the presence of two dissociable protons in DEH. The proton–ligand and metal–ligand formation constants decrease with the increase in temperature. At a particular temperature, the trend in the stability constants of the metal complexes is in the order: $Pr(III) < Nd(III) < Gd(III) > Tb(III) < Ho(III)$. Complexation reactions are spontaneous, exothermic, and of unfavorable entropy. The ligand has no sensitizing effect on Tb(III) luminescence, and it coexists as a mixture of inner and outer sphere complexes in ethanolic medium. The potentiometric study indicates the formation of both 1:1 and 1:2 metal–ligand complexes, while the photoluminescence study shows that there is interaction between DEH and the Ln(III) ions, which is confirmed by the isolation and characterization of the Tb(III) complex.

■ ASSOCIATED CONTENT

S Supporting Information. Values of n and pL of Ln(III) DEH at 303.15 K and $I = 0.1\text{ mol} \cdot \text{dm}^{-3}$ KNO_3 and FTIR data of DEH and the Tb(III)-DEH complex (Tables 1 and 2, respectively). A thermogram of the complex is shown in Figure 1, keto enol tautomerism of DEH in Figure 2, and a plot of $\log \beta_{DEH}^{Ln}$ vs $1/r$ in Figure 3. This material is available free of charge via the Internet at <http://pubs.acs.org>.

■ AUTHOR INFORMATION

Corresponding Author

*E-mail: yuivah@gmail.com. Tel.: 09402880425. Fax: 0385-2435145.

Funding Sources

Special thanks to University Grants Commission, New Delhi for providing financial assistance to Y.V. under RGNFS.

Notes

†E-mail: lonirk@yahoo.co.uk.

■ ACKNOWLEDGMENT

The authors also acknowledge Central Drug Research Institute, Lucknow for recording NMR and mass spectra of the ligand.

■ REFERENCES

- (1) Buss, J. L.; Kyle, E. A.; Shephard, C.; Ponka, P. Lipophilicity of Analogs of Pyridoxal Isonicotinoyl Hydrazone (PIH) Determines the Efflux of Iron Complexes and Toxicity in K562 Cells. *Biochem. Pharmacol.* **2003**, *65*, 349–360.
- (2) Tossidis, I. A.; Bolos, C. A.; Aslanidis, P. N.; Katsoulos, G. A. Monohalogenobenzoylhydrazones III. Synthesis and Structural Studies of Pt(II), Pd(II) and Rh(III) Complexes of Di-(2-pyridyl)-ketonechlorobenzoyl Hydrazones. *Inorg. Chim. Acta* **1987**, *133*, 275–280.
- (3) Sevim, R.; Güniz, K. S. Biological Activities of Hydrazone Derivatives. *Molecules* **2007**, *12*, 1910–1939.
- (4) Singh, V.; Srivastava, V. K.; Palit, G.; Shanker, K. Coumarin Congeners as Antidepressants. *Arzneim.-Forsch. Drug Res.* **1992**, *42*, 993–996.
- (5) Fox, H. H. The Chemical Approach to the Control of Tuberculosis. *Science* **1952**, *116*, 129–134.
- (6) Sah, P. P. T.; Peoples, S. A. Isonicotinyl Hydrazones as Antitubercular Agents and Derivatives for Identification of Aldehydes and Ketones. *J. Am. Pharm. Assoc.* **1954**, *43*, 513–524.

- (7) Campbell, M. J. M. Transition Metal Complexes of Thiosemicarbazide and Thiosemicarbazones. *Coord. Chem. Rev.* **1975**, *15*, 279–319.
- (8) Agarwal, R. K.; Sarin, R. K. Synthesis and Characterization of some Lanthanide(III) Perchlorate Complexes of Hydrazones of Isonicotinic Acid Hydrazide. *Polyhedron* **1993**, *12*, 2411–2415.
- (9) Richardson, D. R.; Bernhardt, P. V. Crystal and Molecular Structure of 2-hydroxy-1-naphthaldehyde Isonicotinoyl Hydrazone (INH) and its Iron (III) complex: an Iron Chelator with Anti-tumour Activity. *J. Biol. Inorg. Chem.* **1999**, *4*, 266–273.
- (10) Sharma, K. K.; Singh, R.; Fahmi, N.; Singh, R. V. Synthesis, Coordination Behavior, and Investigations of Pharmacological Effects of Some Transition Metal Complexes with Isoniazid Schiff Bases. *J. Coord. Chem.* **2010**, *63* (17), 3071–3082.
- (11) Louie, A. Y.; Meade, T. J. Metal Complexes as Enzyme Inhibitors. *Chem. Rev.* **1999**, *99*, 2711–2734.
- (12) Yang, Z. Y.; Yang, R. D.; Li, F. S.; Yu, K. B. Crystal structure and antitumour activity of some rare earth metal complexes with Schiff Base. *Polyhedron* **2000**, *19*, 2599–2604.
- (13) Buss, J. L.; Neuzil, J.; Ponka, P. Oxidative stress mediates toxicity of pyridoxal isonicotinoyl hydrazone analogs. *Arch. Biochem. Biophys.* **2004**, *421*, 1–9.
- (14) Sommer, L.; Maung-Gyee, W. P.; Ryan, D. E. Heterocyclic Hydrazones of o-hydroxyaldehyde as Analytical Reagents. *Ser. Fac. Sci. Nat. Univ. Purkyntiana* **1972**, *2* (6), 115–128.
- (15) Agarwal, R. K.; Singh, L.; Sharma, D. K.; Singh, R. Synthesis, Spectral and Thermal Investigations of some Oxovanadium(IV) complexes of Hydrazones of Isonicotinic acid Hydrazide. *Turk. J. Chem.* **2005**, *29* (3), 309–316.
- (16) Rao, T. R.; Lonibala, R. K. X-ray Diffraction Studies of Zn(II) Complexes of Furfuralidine Isonicotinoyl Hydrazone. *Cryst. Res. Technol.* **1991**, *26*, K1–K4.
- (17) Singh, G.; Shastri, P. S. S. J.; Lonibala, R. K.; Rao, T. R. Coordination Behavior of Pyridoxal Isonicotinoyl Hydrazone Towards some 3d-metal Ions. *Synth. React. Inorg. Met.-Org. Chem.* **1992**, *22* (7), 1040–1059.
- (18) Sharmeli, Y.; Lonibala, R. K. Thermodynamics of the Complexation of N(Pyridin-2-ylmethylene)Isonicotinohydrazide with Lighter Lanthanides. *J. Chem. Eng. Data* **2009**, *54* (1), 28–34.
- (19) Sharmeli, Y.; Lonibala, R. K. Complex Formation of N'-[4-(dimethylamino)phenyl]methylene Isonicotinohydrazide with Lanthanide Ions in Water-Dioxane Medium and the Associated Thermodynamics. *Asian J. Chem.* **2010**, *22* (10), 7541–7550.
- (20) Lajunen, L. H. J.; Portanova, R.; Piispanen, J.; Tolazzi, M. Critical Evaluation of Stability Constants for α -Hydroxycarboxylic Acid Complexes with Protons and Metal Ions and the Accompanying Enthalpy Changes - Part I: Aromatic ortho-Hydroxycarboxylic acids. *Pure Appl. Chem.* **1997**, *69* (2), 329–338.
- (21) Beck, M. T. Critical Evaluation of Equilibrium Constants in Solution Stability of Metal Complexes. *Pure Appl. Chem.* **1977**, *49*, 127–135.
- (22) Hemmila, I.; Laitala, V. Progress in Lanthanides as Luminescent Probes. *J. Fluoresc.* **2005**, *15* (4), 529–542.
- (23) Gunnlaugsson, T.; Leonard, J. P. Responsive Lanthanide Luminescent Cyclen Complexes: from Switching/Sensing to Supramolecular Architectures. *Chem. Commun.* **2005**, 3114–3131.
- (24) Bunzli, J. C. G.; Choppin, G. R. *Lanthanides Probes in Life, Chemical and Earth Sciences, Theory and Practice*; Elsevier: New York, 1989.
- (25) Eliseeva, S. V.; Bunzli, J. C. G. Lanthanide luminescence for functional materials and bio-sciences. *Chem. Soc. Rev.* **2010**, *39*, 189–227.
- (26) Meares, C. F.; Wensel, T. G. Metal Chelates as probes of Biological Systems. *Acc. Chem. Res.* **1984**, *17*, 202–209.
- (27) Soini, E.; Lovgren, T. Time-resolved Fluorescence of Lanthanide Probes and Applications in Biotechnology CRC. *Crit. Rev. Anal. Chem.* **1987**, *18*, 105–154.
- (28) Simon, P. F. The Therapeutic Application of Lanthanides. *Chem. Soc. Rev.* **2006**, *35*, 524–533.
- (29) Richardson, F. S. Terbium (III) and Europium (III) Ions as Luminescent Probes and Stains for Biomolecular Systems. *Chem. Rev.* **1982**, *82*, 541.
- (30) Irving, H. M.; Rossotti, H. S. The Calculation of Formation Curves of Metal Complexes from pH- Titration Curves in Mixed Solvents. *J. Chem. Soc.* **1954**, *30A*, 2904–2910.
- (31) Irving, H. M.; Rossotti, H. S. Methods for Computing Successive Stability Constants from Experimental Formation Curves. *J. Chem. Soc.* **1953**, 3397, 3405.
- (32) Jeffery, G. H.; Bassett, J.; Mendham, J.; Denny, R. C. *Vogel's Textbook of Quantitative Analysis*, 5th ed.; Wiley: New York, 1994.
- (33) Welcher, F. J. *The Analytical Uses of Ethylenediaminetetraacetic Acid*; Von Nostrand: Princeton, NJ, 1965.
- (34) Bjerrum, J. *Metal Ammine Formation in Aqueous Solution*; P. Hasse and Sons: Copenhagen, 1941.
- (35) El-Sherbiny, M. F. Potentiometric and Thermodynamic Studies of 2-Thioxothiazolidin-4-one and its Metal Complexes. *Chem. Pap.* **2005**, *59* (5), 332–335.
- (36) Sekhon, B. S.; Chopra, S. L. A Thermodynamic Study of the Complexation Reaction for Some Amino Acids with Cerium (III) and Yttrium (III). *Thermochim. Acta* **1973**, *7*, 151–157.
- (37) Young, I. K.; Sung, N. C.; Chi, G. S. Thermodynamic Parameters on the Complexation of Trivalent Lanthanide Ions by Cyclopentanecarboxylate in Aqueous Solution. *Bull. Korean Chem. Soc.* **2001**, *22* (6), 641–643.
- (38) Biradar, N. S.; Kulkarni, V. H. A Spectroscopic Study of Tin(IV) Complexes with Multidentate Schiff Bases. *J. Inorg. Nucl. Chem.* **1971**, *33*, 3781–3786.
- (39) Jeragh, B.; Al-Wahaib, D.; El-Sherif, A. A.; El-Dissouky, A. Potentiometric and Thermodynamic Studies of Dissociation and Metal Complexation of 4-(3-Hydroxypyridin-2-ylimino)-4-phenylbutan-2-one. *J. Chem. Eng. Data* **2007**, *52*, 1609–1614.
- (40) Ettai, P.; Charyulu, K. J.; Omprakash, K. L.; Chandra Pal, A. V.; Reddy, M. L. N. Formation of Some Binary and Ternary Complexes of Lanthanides with 8-Formyl-7-Hydroxy-4-Methyl-2H-[1]Benzopyran-2-one. *Indian J. Chem.* **1985**, *24A*, 890–892.
- (41) Piszczek, G.; Maliwal, B. P.; Gryczynski, I.; Dattelbaum, J.; Lakowicz, J. R. Multiphoton Ligand-Enhanced Excitation of Lanthanides. *J. Fluoresc.* **2001**, *11* (2), 2001.
- (42) Stein, G.; Wurzburg, E. Energy Gap Law in the Solvent Isotope Effect on Radiationless Transitions of Rare Earth Ions. *J. Chem. Phys.* **1975**, *62*, 208–213.
- (43) Ermolaev, V. L.; Sveshnikova, E. B. A Mechanism of Non-radiative Transitions in Lanthanide Ions and the Number of Water Molecules in Their First Coordination Sphere. *Opt. Spectrosc.* **2003**, *95* (6), 908–913.
- (44) Salama, S.; Richardson, F. S. Influence of Ligand N-H Oscillators vs. Water O-H Oscillators on the Luminescence Decay Constants of Terbium (III) Complexes in Aqueous Solution. *J. Phys. Chem.* **1980**, *84*, 512–517.
- (45) Beeby, A.; Clarkson, I. M.; Dickins, R. S.; Faulkner, S.; Parker, D.; Royle, L.; de Sousa, A. S.; Williams, J. A. G.; Woods, M. Non-radiative Deactivation of the Excited States of Europium, Terbium and Ytterbium Complexes by Proximate Energy-matched OH, NH and CH Oscillators: An Improved Luminescence Method for Establishing Solution Hydration States. *J. Chem. Soc., Perkins Trans. 2* **1999**, 493–503.
- (46) Wang, Z. M.; Choppin, G. R.; Dibernado, P. L.; Zanonato, P. L.; Portanova, R. P.; Tolazzi, M. J. Luminescence Spectroscopic Study of Europium(III) and Terbium(III) with Ethylenediamine in Dimethyl Sulfoxide. *J. Chem. Soc., Dalton Trans.* **1993**, 2791–2796.
- (47) Iglesias, C. P.; Elhabiri, M.; Hollenstein, M.; Bunzli, J. C. G.; Piguet, C. Effect of a Halogenide Substituent on the Stability and Photophysical Properties of Lanthanide Triple-stranded Helicates with Ditopic Ligands derived from Bis(benzimidazolyl)pyridine. *J. Chem. Soc., Dalton Trans.* **2000**, 2031–2043.
- (48) Choppin, G. R.; Strazik, W. F. Complexes of Trivalent Lanthanide and Actinide Ions. I. Outer-Sphere Ion Pairs. *Inorg. Chem.* **1965**, *4*, 1250–1254.

(49) Linfeng, R. Guaxin, tian. Complexation of Lanthanides with Nitrate at Variable Temperature: Thermodynamics and coordination Modes. *Inorg. Chem.* **2009**, *48*, 964–970.

(50) Geary, W.J. The use of Conductivity Measurements in Organic Solvents for the Characterisation of Coordination Compounds. *Coord. Chem. Rev.* **1971**, *7*, 81–122.

(51) Makode, J. T.; Yaul, A. R.; Bhadange, S. G.; Aswar, A. S. Physicochemical Characterization, Thermal, and Electrical Conductivity Studies of some Transition Metal Complexes of Bis-Chelating Schiff Base. *Russ. J. Inorg. Chem.* **2009**, *54* (9), 1372–1377.